Temperature Dependence of Impurity Induced EFG's in Extremely Diluted CuB*

G. Sulzer**, B. Ittermann, E. Diehl, B. Fischer, H.-P. Frank, E. Jäger, W. Seelinger, H.-J. Stöckmann, H. Ackermann

Fachbereich Physik und Wissenschaftliches Zentrum für Materialwissenschaften, Universität Marburg, Renthof 5, 35032 Marburg, Germany

Z. Naturforsch. **49a**, 354–360 (1994); received July 23, 1993

The temperature dependence of impurity induced EFG's around implanted ^{12}B ions in Cu was measured for two lattice locations using the β-NMR method. The induced EFG at the nearest neighbouring host atoms decreases with increasing temperature for the case of ^{12}B stopped on interstitial sites, whereas the opposite temperature behaviour was found if ^{12}B is situated in substitutional sites.

Key words: NMR, β radiation detected, Cross relaxation, Electric field gradient, Temperature dependence of EFG, Impurity induced EFG.

1. Introduction

This contribution deals with the measurement of temperature dependences of electric field gradients (EFG's) induced at the sites of the surrounding Cu host nuclei by isolated ^{12}B impurities. The applied technique is β radiation detected cross relaxation (CR) of spin polarized ^{12}B probe nuclei ($\tau_\beta = 29$ ms, $I = 1$) implanted into Cu single crystals.

Radioactive probe nuclei can often be prepared in states having a very high degree of spin polarization compared to the host spin system. If this is the case, they represent an ideal spin ensemble to study CR in connection with the host spin system. In the present context we speak of CR processes, whenever energy of probe spins I is transferred to the surrounding host spins S by direct dipolar coupling, leading to an additional depolarization rate of the I system [1]. Due to the condition of energy conservation, CR is also an appropriate technique to study static interactions like the electric quadrupole interaction. This fact will be used below.

There exist only a few measurements in the field of impurity or probe induced EFG's: Working on stable isotopes, Jensen and co-workers applied NMR in single crystals [2, 3] and Minier and co-workers NQR field-cycling in polycrystals [4, 5] to measure impurity induced EFG's in metals. A theoretical overview has been given by Prakash [6]. Measurements on crystal EFG's in non-cubic metals and of their temperature dependence by use of radioactive probes have been reported by Witthuhn et al. [7]. Applying perturbed angular correlations with ^{111}In as a probe, Deicher et al. [8] have determined the magnitude and the temperature behaviour of the EFG induced by a monovacancy at the site of the probe atom in cubic Cu, Ag and Au. In the first CR experiment using β active probes, Fujara et al. [9] succeeded in deducing the crystal EFG at the Nb site in $LiNbO_3$ by observing ^{8}Li–^{93}Nb cross processes. In a recent work Ittermann et al. [10] were able to determine the EFG at first (nn) and second (nnn) nearest-neighbour-positions in Vanadium induced by ^{12}B impurities located in interstitial or in substitutional sites. However, the temperature dependence of these EFG's was not measured in that work.

To our knowledge there exist only two measurements of the temperature dependence of impurity induced EFG's. Performing CR measurements on ^{12}B in Al, Cyamukungu et al. [11] found a $T^{3/2}$ behaviour for the ^{12}B induced EFG at nn and nnn Al host nuclei. The second experiment is the present one reporting the temperature dependence of the EFG's at Cu host nuclei induced by ^{12}B impurities occuring in two different lattice locations.

* Presented at the XIIth International Symposium on Nuclear Quadrupole Resonance, Zürich, July 19–23, 1993.

** Present address: Hahn-Meitner-Institut Berlin GmbH, Bereich Schwerionenphysik, Glienicker Str. 100, 14109 Berlin, Germany.

Reprint requests to G. Sulzer, Hahn-Meitner-Institut Berlin GmbH, Bereich Schwerionenphysik, Glienicker Str. 100, 14109 Berlin, Germany.

0932-0784 / 94 / 0100-0354 $ 01.30/0. – Please order a reprint rather than making your own copy.

2. Experimental and basics of the CR technique

In this work the β emitter ^{12}B ($\tau_\beta = 29$ ms, $I=1$, $\gamma/2\pi = 7.644$ MHz/T) was used as probe: ^{12}B nuclei were produced by the nuclear reaction ^{11}B (d,p) ^{12}B with a 1.5 MeV deuteron beam in a thin boron target foil. The ^{12}B ions ejected from the target were polarized by selecting a recoil angle ($45 \pm 6°$) and implanted with broadly distributed energies (0 ... 450 keV) into the single crystalline Cu sample. This led to a rather homogeneous depth distribution extending to about 1 μm. Due to the very low implantation flux of $\sim 10^5$ cm^{-2} s^{-1}, the local ^{12}B concentration never exceeded 10^7 cm^{-3}. Thus, the probe nuclei are completely isolated from each other and any direct $I-I$ interaction is excluded.

The polarization degree obtained by the nuclear reaction was of the order of 10%, and the stationary polarization P_I of the I-spin probes was measured via the 0-π asymmetry of the β-decay radiation [12]. A more detailed description of the experimental design and the experiment is given in [13].

CR between ^{12}B (I spin) and a neighbouring Cu nucleus (S spin, $S=3/2$, $\gamma/2\pi(^{63}\text{Cu}) = 11.284$ MHz/T, $\gamma/2\pi(^{65}\text{Cu}) = 12.089$ MHz/T) is caused by their direct dipole-dipole interaction. It may lead to mutual spin flips, provided energy is conserved. If only Zeeman interaction is present for both of the spins involved, I and S, energy conservation holds only in the region of very small external magnetic field, where the dipolarly broadened line profiles of probe and host overlap. However, if additionally quadrupole interactions are present for at least one of the two spin species, the coincidences of the level splittings can also occur at higher B values. In Fig. 1 a we demonstrate the case of pure Zeeman interaction for the I spins, but simultaneous Zeeman plus electric quadrupole interactions for the S spins. Because of the polarization transfer from the I to the S system, the $P_I(B)$ curve displays resonance-like dips at nonzero B values when the ^{12}B spin polarization is registered versus B (Figure 1 c). These B values depend on the relative strengths of magnetic and electric interaction. Thus cross-relaxation measurements can be used to determine the energy levels of the involved spins and therefore the values of the EFG's. Moreover, it is possible to deduce unambiguously the lattice sites of the impurity from the symmetry of the induced EFG.

Since no rf irradiation is necessary in these experiments and since the polarization stems from a nuclear reaction, this kind of measurement may be successful in otherwise unfavourable cases: Single crystals of metals (skin effect), and experiments at high temperature or small B fields (low Boltzmann polarization).

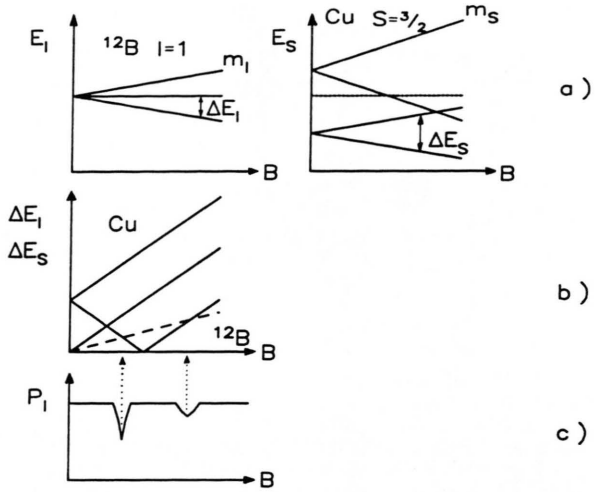

Fig. 1. Principle of the cross-relaxation process. a) Energy diagrams $E_I(B)$ and $E_S(B)$ of two spin species $I=1$ and $S=3/2$ with pure Zeeman interaction for the I spins and simultaneous Zeeman and quadrupole interactions for the S spins with asymmetry parameter $\eta=0$ and $\boldsymbol{B} \parallel eq$. b) Transition energies ΔE_I and ΔE_S of spins I and S versus B. Two crossovers occur at $B \neq 0$. c) Polarization of the I-spin system versus B. $P_I(B)$ shows resonance-like dips at the crossover B values.

Next we consider the ^{12}B-Cu system in more detail. Since Cu has the fcc structure, both interstitial and substitutional lattice sites can possess cubic surroundings. Therefore – and this was indeed confirmed by β-NMR spectra [14] – we are allowed to consider pure magnetic interaction for the ^{12}B impurities. The transition energy ΔE_I between the Zeeman levels of the probe nuclei can thus be written as

$$\Delta E_I = E_I(m_I \rightarrow m_I - 1) = \gamma_I \hbar B . \tag{1}$$

γ_I denotes the gyromagnetic ratio of the I spins. Since the Cu S spins are neighbouring a ^{12}B impurity which disturbs their cubic surroundings, they exhibit magnetic as well as electric interactions. Therefore the $\Delta m = 1$ transition energy ΔE_S in the S-spin system is given in first order perturbation theory by

$$\begin{aligned} \Delta E_S &= E_S(m_S \rightarrow m_S - 1) \\ &= \gamma_S \hbar B - \frac{3e^2qQ}{8S(2S-1)} \\ &\quad \cdot (3\cos^2\vartheta - 1 + \eta \sin^2\vartheta \cos 2\varphi) \cdot (2m_S - 1) . \end{aligned} \tag{2}$$

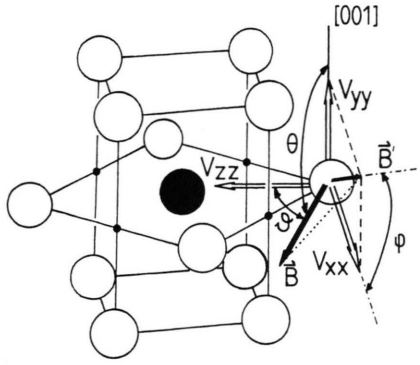

Fig. 2. Definition of the angles used for the description of the quadrupole interaction in the case of substitutionally located ^{12}B in fcc Cu. The crystal orientation with respect to the external $\boldsymbol{B}$ field is determined by the angle Θ between the [001] axis and $\boldsymbol{B}$. The angles ϑ and φ define the orientation of the EFG tensor relative to $\boldsymbol{B}$. The largest component V_{zz} of the tensor is assumed to be parallel to the line connecting probe and host nucleus and encloses with $\boldsymbol{B}$ the angle ϑ. In the case of an asymmetry parameter $\eta \neq 0$, the angle φ gives the orientation of the projection $\boldsymbol{B}'$ of the direction of $\boldsymbol{B}$ into the $V_{xx}-V_{yy}$ plane. •: ^{12}B probe; ○: Cu host.

γ_S is the gyromagnetic ratio of the S spins, and $e^2 qQ/h$ denotes the quadrupole coupling constant (qcc) containing the quadrupole moment Q of the S nuclei and the maximum component $V_{zz}=eq$ of the impurity induced EFG. η is the asymmetry parameter of the EFG tensor. ^{12}B populates two lattice positions, namely the octahedral interstitial site (OI) and the substitutional lattice site (S). From simple symmetry considerations follows $\eta=0$ for the OI, but $\eta\neq 0$ for the S. Furthermore, in (2) the angle ϑ describes the orientation of the EFG-main axis V_{zz} with respect to the direction of $\boldsymbol{B}$, and φ is the angle between the projection of $\boldsymbol{B}$ onto the $V_{xx}-V_{yy}$ plane of the EFG tensor and V_{xx} (Figure 2).

CR dips can occur whenever the condition $\Delta E_S=\Delta E_I$ is fulfilled, and we get from (1) and (2) for the corresponding values of B

$$B_{m_S}=\frac{2\pi}{\gamma_S-\gamma_I}\cdot\frac{3e^2qQ/h}{8S(2S-1)} \cdot(3\cos^2\vartheta-1+\eta\sin^2\vartheta\cos 2\varphi)\cdot(2m_S-1)\,. \tag{3}$$

For the following we note that in (3) the term containing the asymmetry parameter vanishes not only for $\eta=0$ but also if the special orientation $V_{zz}\parallel\boldsymbol{B}$ (i.e. $\vartheta=0°$) is chosen.

Whether CR processes can be observed or not depends on the strength of the nondiagonal terms of the dipole-dipole interaction. The full CR process can be described by the solution of the Liouville equation

$$\dot{\varrho}=\frac{i}{\hbar}\cdot[\varrho,\mathscr{H}]\,, \tag{4}$$

where ϱ is the density matrix of the system consisting of I and S spins and $\mathscr{H}$ is the complete Hamiltonian [1]

$$\mathscr{H}=\mathscr{H}_I+\Sigma_i\,\mathscr{H}_{S_i}+\mathscr{H}_{\mathrm{DD}}\,. \tag{5}$$

Here $\mathscr{H}_I$ and $\mathscr{H}_{S_i}$ are the single particle operators for I and S spins respectively, each describing Zeeman and possible additional quadrupolar energies. $\mathscr{H}_{\mathrm{DD}}$ takes into account the various contributions of the dipole-dipole interaction. For further theoretical details we refer to [15]. Here we only mention that the theoretical P_I (B) curves can be calculated using (4) and (5). Fitting the calculations to the measured CR spectra yields the lattice sites of ^{12}B and the corresponding EFG's at the nn host nuclei.

3. Measurements and results

CR spectra of ^{12}B in Cu were measured as functions of B between zero and 0.4 T in the temperature range 300–700 K at various crystal orientations. Figure 3 shows two examples measured at 480 K for the two orientations $\boldsymbol{B}\parallel\langle 110\rangle$ and $\boldsymbol{B}\parallel\langle 100\rangle$. In both spectra several resonance-like CR dips appear. Because of the different magnetic dipole and electric quadrupole moments of the isotopes ^{63}Cu and ^{65}Cu, two different sets of B values occur. For example, CR dips for ^{12}B–^{63}Cu cross processes appear at $B\simeq 265$ mT (for $\boldsymbol{B}\parallel\langle 110\rangle$) and $B\simeq 185$ mT (for $\boldsymbol{B}\parallel\langle 100\rangle$), but at $B\simeq 200$ mT ($\boldsymbol{B}\parallel\langle 110\rangle$) and $B\simeq 135$ mT ($\boldsymbol{B}\parallel\langle 100\rangle$) for the pair ^{12}B–^{65}Cu. The decrease of polarization in the CR spectra for small B values may be due to hyperfine interaction in flight of the ^{12}B ions leaving the target foil and to CR processes with neighbouring Cu nuclei in higher shells.

Comparing the experimental spectra with theoretical ones calculated for different lattice locations of ^{12}B in Cu, we deduced earlier that ^{12}B takes up two different sites with high symmetry: CR spectra showing up between room temperature and 410 K correspond to ^{12}B in OI [16]. The corresponding induced qcc at the nearest neighbouring Cu nuclei amounts at 310 K to

$$\begin{aligned}|e^2qQ(^{63}\mathrm{Cu})/\mathrm{h}|&=4.029(5)\ \mathrm{MHz}\,,\\ |e^2qQ(^{65}\mathrm{Cu})/\mathrm{h}|&=3.724(11)\ \mathrm{MHz}\,,\end{aligned} \tag{6}$$

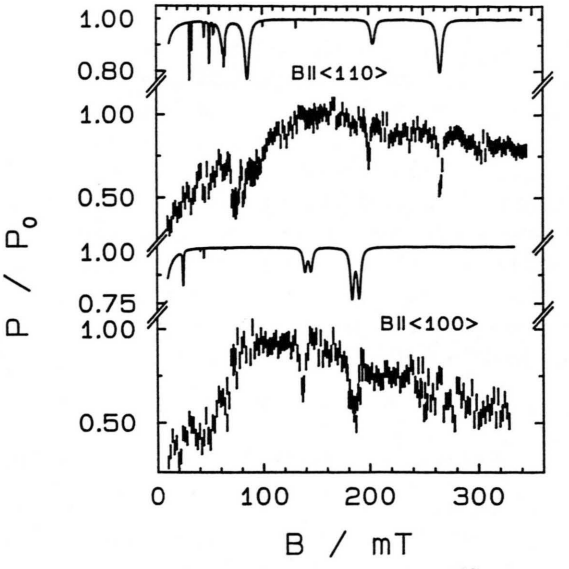

Fig. 3. Measured and calculated CR spectra of ^{12}B in Cu at $T=480$ K for the two orientations $\boldsymbol{B}\|\langle 110\rangle$ and $\boldsymbol{B}\|\langle 100\rangle$. The two prominent high-field dips in each spectrum correspond to cross processes of substitutionally located ^{12}B with ^{63}Cu and ^{65}Cu host spins, respectively, in the first neighbour shell.

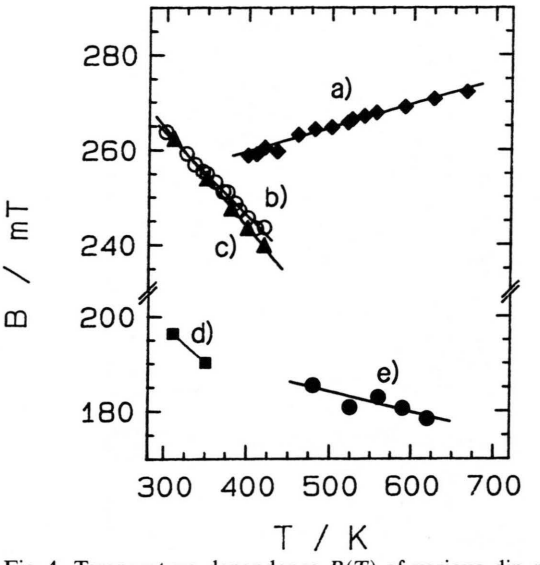

Fig. 4. Temperature dependence $B(T)$ of various dip positions (notation: ^{12}B site; interacting host isotope; crystal axis $\|\boldsymbol{B}$; ϑ as defined in Figure 2). a) (S; ^{63}Cu; $\langle 100\rangle$; 0°), b) (OI; ^{63}Cu; $\langle 110\rangle$; 90°), c) (OI; ^{63}Cu; $\langle 100\rangle$; 90°), d) (OI; ^{65}Cu; $\langle 100\rangle$; 90°), e) (S; ^{63}Cu; $\langle 100\rangle$; 90°).

with $\eta=0$. The ratio of these qcc's resulting from independent fits yields the ratio of the quadrupole moments of both Cu isotopes. We obtained $|Q(^{63}\mathrm{Cu})/Q(^{65}\mathrm{Cu})|=1.0819(35)$, which agrees within the error bars with the literature value [17]. These values for both qcc's and their ratio presented here differ slightly within the given errors from those reported earlier [15, 16] because of better statistics and refined analysis.

Between 430 K and 670 K the measured CR spectra can theoretically be described only by assuming the probes in the S position. From the fit we get for the corresponding induced qcc's at nn-Cu nuclei at 480 K

$$\begin{aligned} |e^2qQ(^{63}\mathrm{Cu})/\mathrm{h}| &= 2.006(37)\ \mathrm{MHz}\,, \\ |e^2qQ(^{65}\mathrm{Cu})/\mathrm{h}| &= 1.856(34)\ \mathrm{MHz}\,. \end{aligned} \tag{7}$$

Here the known ratio of quadrupole moments $|Q(^{63}\mathrm{Cu})/Q(^{65}\mathrm{Cu})|=1.0806(3)$ [17] was used in the fitting procedure to obtain both qcc's and the asymmetry parameter with higher accuracy. Contrary to the OI case, substitutional ^{12}B induces a nonaxially symmetric EFG at its nn-host nuclei and the asymmetry parameter amounts at 480 K to

$$\eta=0.30\,(5)\,. \tag{8}$$

It should be pointed out again that the CR spectra depend very sensitively upon the orientation of the EFG main axis V_{zz} with respect to $\boldsymbol{B}$. In Fig. 3, e.g., in the spectrum corresponding to the crystal orientation $\boldsymbol{B}\|\langle 110\rangle$ the CR dip at $B\simeq 265$ mT can be assigned to $\vartheta=0°$, whereas for the crystal orientation $\boldsymbol{B}\|\langle 100\rangle$ the CR dip at $B\simeq 185$ mT has $\vartheta=90°$.

In Fig. 4 the temperature dependence of the position of the CR dips $B(T)$ is shown for both ^{12}B sites and two crystal orientations. To obtain this dependence, the positions of some prominent dips in the CR spectra were registered for $\boldsymbol{B}\|\langle 110\rangle$ and $\boldsymbol{B}\|\langle 100\rangle$, and for the two ^{12}B positions OI and S. It turned out that for ^{12}B located in OI all observed CR dips shift to lower B values with increasing temperature (curves b), c), and d) in Figure 4). The dips belonging to the S position, however, behave differently depending on the angle ϑ (curves a) and e) in Figure 4).

We first consider the OI case. As can be seen from (3), for $\eta=0$ the dip positions are directly proportional to the qcc for a fixed orientation factor $(3\cos^2\vartheta-1)$. Thus the temperature dependence of the qcc corresponds directly to that of the dip positions $B(T)$. With $Q(^{63}\mathrm{Cu})=-0.220\,(15)$ barn and $Q(^{65}\mathrm{Cu})=-0.204\,(14)$ barn [18] we obtain the $q(T)$ diagram

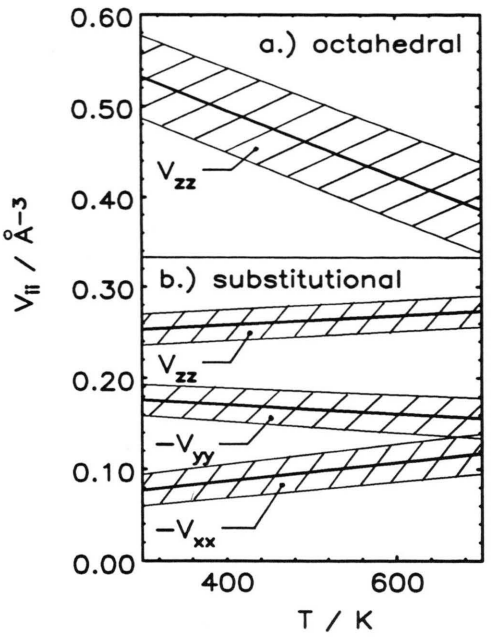

Fig. 5. Temperature dependence of the EFG-tensor components for both lattice locations of ^{12}B in Cu. The hatched areas indicate the errors. a) $V_{zz}(T)$ of the impurity induced EFG at nn Cu host nuclei in the OI case. b) $V_{zz}(T)$, $V_{xx}(T)$, and $V_{yy}(T)$ components of the impurity induced EFG at nn Cu host nuclei in the S case.

shown in Figure 5a. To achieve a high accuracy, the measured dip positions $B(T)$ were first approximated by a linear fit and then the temperature dependence of q was evaluated as

$$q(T)=0.641\,(44)\,\text{Å}^{-3}-3.65\,(27)\cdot 10^{-4}\,\text{Å}^{-3}\cdot T/\text{K}\,. \tag{9}$$

Next we discuss the case where ^{12}B takes up the S position. Here, the situation is complicated by the additional T dependent term $\eta(T)\sin^2\vartheta\cos 2\varphi$ in (3). As was already mentioned above, the behaviour of $B(T)$ is different for $\boldsymbol{B}\parallel\langle 110\rangle$ and $\boldsymbol{B}\parallel\langle 100\rangle$ in the case of substitutional ^{12}B: For CR spectra taken under the crystal orientation $\boldsymbol{B}\parallel\langle 110\rangle$ we observed a shift of the dip positions to higher B values with increasing temperature, whereas the opposite behaviour was found for CR spectra for the orientation $\boldsymbol{B}\parallel\langle 100\rangle$. From (3) we obtain for the two orientations

$$\boldsymbol{B}\parallel\langle 110\rangle,\ \vartheta=0^\circ:\ B_{3/2}=\frac{2\pi}{\gamma_S-\gamma_I}\cdot\frac{12e^2qQ}{8S(2S-1)h}, \tag{10a}$$

$$\boldsymbol{B}\parallel\langle 100\rangle,\ \vartheta=90^\circ: \tag{10b}$$

$$B_{-1/2}=\frac{2\pi}{\gamma_S-\gamma_I}\cdot\frac{6e^2qQ}{8S(2S-1)h}\cdot(1+\eta)\,.$$

Favourably, (10a) does not contain η, and again $B(T)$ directly reflects the temperature dependence of $q(T)$. In (10b), however, both temperature dependent quantities q and η appear. Thus we conclude that the increase of q with temperature leading to an increase of $B(T)$ as observed for the $\boldsymbol{B}\parallel\langle 110\rangle$ spectra is overbalanced in the case $\boldsymbol{B}\parallel\langle 100\rangle$ by the decrease of $\eta(T)$, leading totally to a decrease of $B(T)$. Thus we calculated the temperature dependence of $q(T)$ and subsequently also of $\eta(T)$ from the CR spectra corresponding to (10a) and (10b), respectively. The results obtained for ^{12}B in the S position are

$$q(T)=0.238(17)\,\text{Å}^{-3}+4.97(39)\cdot 10^{-5}\,\text{Å}^{-3}\cdot T/\text{K}\,, \tag{11a}$$

$$\eta(T)=0.58\,(13)-6.3\,(11)\cdot 10^{-4}\cdot T/\text{K}\,. \tag{11b}$$

With the definition $\eta=(V_{xx}-V_{yy})/V_{zz}$, and the Laplace equation $V_{xx}+V_{yy}+V_{zz}=0$, the temperature dependences of $V_{xx}(T)$ and $V_{yy}(T)$ were determined from those for η and q and are shown in Fig. 5b together with $V_{zz}=eq$. The three EFG-tensor components behave differently: In Fig. 5b, $|V_{zz}|$ and $|V_{xx}|$ increase with increasing temperature whereas $|V_{yy}|$ decrease, leading to higher axial symmetry of the EFG tensor with increasing temperature.

4. Discussion

In the past, studies of the temperature dependences of EFG's in metals have in most cases been restricted to the measurements of EFG's at substitutional sites. These EFG's were either probed by a host nucleus in an unperturbed system with non-cubic symmetry or by a substitutional impurity [19, 20]. The majority of the experimental results has been obtained by NQR and PAC techniques. These experiments often found the well-known $T^{3/2}$-temperature dependence $q(T)=q(0)\,(1-b\,T^{3/2})$, with $\mathrm{d}q/\mathrm{d}T<0$ [19, 21], for the EFG's. All approaches to understand this behaviour had to consider, of course, that the primary reason for the existence of these intrinsic EFG's are the low symmetries of the charge distributions in the unperturbed host lattices. Explanations of $\mathrm{d}q/\mathrm{d}T$ therefore had to deal with mechanisms altering the nuclear and electronic coordinates of the whole crystal, e.g. due to phonons. To discuss temperature effects on EFG's in this work, however, we have to keep in mind that here the EFG's are created by impurities, i.e. the ^{12}B nuclei, and act on host nuclei on lattice

sites with otherwise perfect cubic symmetry. If we are interested in dq/dT of such impurity induced EFG's, we obviously have to look for the temperature dependence of those mechanisms creating these EFG's in the first place. In general the situation is completely different for impurity induced EFG's and intrinsic EFG's, and a priori there is no reason to expect the same behaviour.

It is clearly beyond the scope of this paper to report in any detail the current status of the theories for impurity induced EFG's in metals, but in the following discussion we would like to sketch some rough ideas how our experimental findings might be understood. Most theoretical works on that topic, reviewed for instance in [6, 22] calculate two separate contributions to the total EFG, namely the so-called size and valence EFG's, q_s and q_v, respectively. The origin of q_s is the rearrangement of the host ions close to the impurity, leading to a locally non-cubic symmetry at any other site than the center of the perturbation. q_v is caused by the charge excess or depletion due to the, in general, different impurity valence. While q_s might be seen as a counterpart to the intrinsic EFG's in non-cubic metallic host structures, there is no direct analogy to q_v in unperturbed systems.

For the following interpretation the decisive fact is that the total EFG's q_{tot} for the system B in Cu can be interpreted as the sum of two rather independent contributions. From various theoretical works on this problem we see that the relative magnitude as well as the relative sign of calculated size and valence EFG's vary strongly from one probe-host system to the other and, especially for dilute substitutional impurities in Cu, comparable magnitude but opposite signs for q_s and q_v have been calculated [23, 24]. Looking at the two different lattice positions of B in Cu we have two major differences: i) the presumably much stronger lattice distortion around an interstitial impurity and therefore a larger size EFG q_s, ii) the shorter distance between B and nn Cu nuclei in the interstitial case. The change in sign of dq_{tot}/dT when going from the interstitial to the substitutional impurity would then result from the different size EFG's around both sites: the strong compressive strain around the interstitial boron creates a very strong EFG dominating q_{tot} as well as its temperature dependence. Let us assume now, for simplicity, that both contributions individually behave 'regularly', i.e. decrease with temperature like almost all intrinsic EFG's in metals do. Because of the dominating role of q_s we then get $dq_{tot}/dT < 0$ as well, as observed experimentally. Putting our impurity on a substitutional site, however, q_s should decrease considerably in magnitude due to its location on a regular site. So in the case of substitutional *B*, q_s, and q_v might be comparable in magnitude. Additionally, from the results of [23] and [24] it is quite possible for q_s and q_v to have different signs. If the larger EFG contribution happens to decrease more slowly with temperature, we end up with a $dq_{tot}/dT > 0$.

It is quite worthwhile to compare our present results of B in Cu to the recent work of Cyamukunga et al. [11], who studied B induced EFG's at nn and nnn Al host atoms using the same cross-relaxation technique. In the temperature range from 50 to 400 K the induced EFG's at the first and second shell of neighbouring host nuclei decrease with temperature in very good accordance with a $T^{3/2}$ law. In that system B always occupies the octahedral interstitial site. We therefore expect q_s to give the dominating contribution to q_{tot}, and because of the inherent similarity between a size EFG and an intrinsic EFG, this 'intrinsic like' temperature behaviour is not in contradiction to our picture.

We are aware of the speculative character of this interpretation. Our aim, however, was not to present a unique model to explain the data, but only to demonstrate that the temperature dependences of the measured EFG's are not as anomalous as they might seem at a first glance, if only the different origin of impurity induced and intrinsic EFG's is considered. If, on the other hand, we believe our scenario to be the correct description, we can even invert our argumentation. From the positive dq_{tot}/dT around substitutional B in Cu we then would get the experimental result that q_s and q_v have different signs. Extrapolating the calculations of [24] in assuming $|q_s|$ to be the larger contribution we additionally obtain that it is the valence EFG that dominates the temperature dependence of q_{tot}.

Acknowledgement

We gratefully acknowledge the hospitality of the Max-Planck-Institut für Kernphysik in Heidelberg and the support of its technical staff. This work was sponsored by the Bundesministerium für Forschung und Technologie.

[1] A. Abragam, in: The Principles of Nuclear Magnetism, Clarendon Press, Oxford 1961.
[2] B. L. Jensen, R. Nevald, and D. Ll. Williams, J. Phys. **F2,** 169 (1972).
[3] R. Nevald, B. L. Jensen, and P. B. Fynbo, J. Phys. **F4,** 1320 (1974).
[4] G. Grüner and M. Minier, Adv. Physics **26,** 231 (1977).
[5] M. Minier and C. Minier, Phys. Rev. **B22,** 21 (1980).
[6] S. Prakash, Hyp. Int. **24–26,** 491 (1985).
[7] W. Witthuhn and W. Engel, in: Hyperfine Interactions of Radioactive Nuclei; Topics in Current Physics vol. 31, ed. J. Christiansen, Springer, Berlin 1983.
[8] M. Deicher, E. Recknagel, and Th. Wichert, Hyp. Int. **10,** 675 (1981).
[9] F. Fujara, H.-J. Stöckmann, H. Ackermann, W. Buttler, K. Dörr, H. Grupp, P. Heitjans, G. Kiese, and A. Körblein, Z. Physik **B37,** 151 (1980).
[10] B. Ittermann, K. Bürkmann, E. Diehl, R. Dippel, B. Fischer, H.-P. Frank, E. Jäger, W. Seelinger, G. Sulzer, H. Ackermann, and H.-J. Stöckmann, Z. Physik **B91,** 7 (1993).
[11] M. Cyamukungu, R. Pirlot, L. Grenacs, J. Lehmann, G. S'heeren, R. Coussement, and K. Tompa, Contribution D5-009 presented at the 9th. Int. Conf. on Hyperfine Interactions, August 17–21, 1992, Osaka, Japan.
[12] H. Ackermann, P. Heitjans, and H.-J. Stöckmann, in: Hyperfine Interactions of Radioactive Nuclei; Topics in Current Physics Vol. 31, ed. J. Christiansen, Springer, Berlin 1983, p 291.
[13] E. Jäger, B. Ittermann, G. Sulzer, K. Bürkmann, B. Fischer, H.-P. Frank, H.-J. Stöckmann, and H. Ackermann, Z. Physik **B80,** 87 (1990).
[14] R. E. McDonald and T. K. McNab, Phys. Lett. **63A,** 177 (1977).
[15] H.-J. Stöckmann, E. Jäger, G. Sulzer, B. Ittermann, H. Ackermann, E. Diehl, R. Dippel, B. Fischer, H.-P. Frank, and W. Seelinger, Hyp. Int. **49,** 235 (1989).
[16] E. Jäger, B. Ittermann, H.-J. Stöckmann, K. Bürkmann, B. Fischer, H.-P. Frank, G. Sulzer, H. Ackermann, and P. Heitjans, Phys. Lett. **123A,** 39 (1987).
[17] G. H. Fuller, J. Phys. Chem. Reference Data **5,** 835 (1976).
[18] P. Raghavan, in: Table of Nuclear Moments, Atomic and Nuclear Data Table, **42** (1989).
[19] E. N. Kaufmann and R. J. Vianden, Rev. Mod. Phys. **51,** 161 (1979).
[20] R. J. Vianden, Hyp. Int. **15/16,** 1081 (1983).
[21] J. Christiansen, P. Heubes, R. Keitel, W. Klinger, W. Loeffler, W. Sandner, and W. Witthuhn, Z. Phys. **B24,** 177 (1976).
[22] T. P. Das and P. C. Schmidt, Z. Naturforsch. **41a,** 47 (1986).
[23] P. L. Sagalyn and M. N. Alexander, Phys. Rev. **B15,** 5581 (1977).
[24] B. Pal, S. Mahajan, S. D. Raj, J. Singh, and S. Prakash, Phys. Rev. **B30,** 3191 (1984).